

Optoelectronically Tuneable Black Silicon Structures for Thermal Camouflage

Aziz Taner Astarlıođlu¹, Nursev Erdođan¹, Cansu Emir², Emre Cořkun^{3,5}, Rařit Turan^{4,5}

¹Turkish Aerospace, Research and Technology Centers, 06980, Ankara, Turkey.

²Department of Electrical and Electronics Engineering, Atilim University, 06830 Ankara, Turkey

³Department of Physics, Canakkale Onsekiz Mart University, 17100 Canakkale, Turkey

⁴Center for Solar Energy Research and Applications (ODTÜ-GÜNAM), Ankara, Turkey

⁵Department of Physics, Middle East Technical University, Ankara, Turkey
TURKEY

aziztaner.astarlioglu@tai.com.tr

ABSTRACT

Camouflage materials and technologies play a crucial role in stealth technologies. Shielding thermal radiation and millimetre radiofrequency (RF) waves are significant in object detection and electromagnetic interference shielding. Black silicon is being utilized to meet the requirements in infrared and RF regimes using texture type and dopant concentration, respectively. In this work, silicon nanowires with the same texture type and different electrical conductivity are fabricated and characterized. First, we investigated the effect of silicon nanowires in the infrared (IR) band. The average transmission of the textured silicon structures is 24% lower than the unprocessed samples in 8 – 14 μm . Structures with the same texture type but different electrical conductivity were also studied. The studies demonstrate that fabricated structures show a comparable transmission in the 8 – 14 μm , while their electromagnetic interference shielding performance in 8 – 12 GHz differs by about 15%.

1.0 INTRODUCTION

Camouflage materials and technologies are a vast field with an increasing range of materials and production methods. Thermal camouflage, however, has been a significant challenge, requiring an ability to control the thermal radiation from the surface. For this reason, the efforts to shield thermal radiation have gained momentum. Besides thermal camouflage, radars, communications, and other avionic systems used in aerospace can malfunction or fail due to external electromagnetic sources. For this reason, electromagnetic interference (EMI) shielding ensures electronic systems can operate reliably and safely together with the thermal camouflage. The electromagnetic radiation emitted by aircraft increases visibility on ground detectors and constitutes an essential source for heat-seeking missiles in infrared and RF regime. In order to develop technology to shield against EM radiation in fighter aircraft, it is necessary to understand the radiation's dependence on the aircraft's shape or flight conditions, such as speed and altitude. While the hot engine components behind the aircraft are a crucial infrared source for mid-wavelength infrared (MWIR) (3 – 5 μm) detectors, the aircraft surface heated by aerodynamic effects at the front is a critical infrared source for long-wavelength infrared (LWIR) (8 – 14 μm) detectors (Kim et al., 2016).

Silicon is widely used in optoelectronic applications such as solar cells, photodiodes, and photodetectors. However, conventional silicon structures cannot shield thermal radiation in infrared bands. Therefore, textured silicon is utilized so that its optical response in the thermal infrared waveband can be tuned for camouflage (Moghimi, Lin and Jiang, 2018). The optical properties of the silicon are determined by the dopant elements and texture type, which results in light trapping (Osminkina et al., 2012, Hu et al., 2003).

The textured structure of silicon and dopant metals provides design flexibility for configuring response in infrared waveband and X-band, respectively. In this study, experimental studies were conducted for textured

silicon structures to understand the behavior in the LWIR (8 – 14 μm) and RF band (8 – 12 GHz). Numerical analyses were also performed in the RF band to compare experimental findings. The results show that the structure's response can be tuned simultaneously in the 8 – 14 μm and 8 – 12 GHz, bands, respectively.

2.0 METHODOLOGY

2.1 Fabrication and Characterization

2.1.1 Fabrication

Semiconductor NanoWire (NW) technology has attracted attention because of its one-dimensional geometry as a solution to lattice mismatch in fabricated heterostructures. There are some advanced methods with sufficient maturity level to produce SiNW, such as vapor-liquid-solid (VLS) (Wagner and Ellis, 1964) laser ablation (Saddiqi et al., 2014), metal-assisted etching (MAE) (Huang et al., 2011), molecular beam epitaxy (MBE) (Fuhrmann et al., 2005), and electron beam evaporation. The VLS method is known as a common technique for epitaxial growth that provides some degree of control over diameter. However, strict control over the diameter and periodicity of SiNW is rather difficult to achieve unless colloidal catalytic metal particles or electron beam lithography are used (Shimizu et al., 2019). The advantage of the laser ablation technique is manifold without needing for a substrate and the composition of the resulting NWs can be varied by changing the composition of the laser target. However, NWs contain both Si and catalyst materials (Schmidt et al., 2009). While MBE and electron beam lithography (EBL) methods can be used with the VLS method and offer the advantage of a very clean environment and, therefore, high reproducibility, the EBL method is limited to the minimum possible SiNW diameter greater than about 40 nm (Wolfsteller et al., 2010).

In this study, the metal-assisted etching (MAE) method was used to produce SiNW, since it allows the fabrication of NWs with reasonably good vertical alignment and spatial uniformity, and it also provides good control over length and diameter of NWs (Zhang, 2014). In addition, MAE is an easy to use and cost-efficient method, making it suitable to produce SiNW in large areas. The superiority of the NW geometry has applied for various combinations of SiNW with several complementary semiconductor materials.

The MAE method was applied to generate NWs using commercial chemicals without further purification. In this process, p-type and n-type, (111) directed, 1–5 Ω cm resistive and 400 μ thick Si wafers were initially cleaned with RCA1 and RCA2 procedures (Kern *et al.*, 1990). The cleaned Si wafers were dipped into the etchant prepared by using silver nitrate (AgNO_3 , 99.5%) and hydrofluoric acid (HF, 38 – 40%) at the molar ratio of 4.6M: 0.02M, at room temperature, for 30 min. The dendrites formed during etching process were removed by nitric acid (HNO_3 , 65%). The etching procedure was finalized by rinsing the samples with deionized water.

2.1.2 Characterization

The electromagnetic properties of the structures in the X-band were characterized using a network analyzer with a waveguide method. Transmission values of the structures were calculated through measured S-parameters. Optical response of the structures in the infrared (IR) band (8 – 14 μm) was determined by Fourier transform infrared (FTIR) spectroscopy analysis. Thicknesses of the SiNWs were determined using SEM.

2.2 Numerical Calculations

Electromagnetic interference shielding properties of the silicon structure was numerically calculated using CST Microwave Studio with a unit cell module in 8.2 – 12.4 GHz. Black silicon was defined as an ohmic sheet in the model as the corresponding wavelength is smaller than the thicknesses of the films in the X-band.

3.0 RESULTS AND DISCUSSION

SEM images of the samples are shown in Figure 1(a), and Figure 1(b), respectively. The results show that sample N-30 and P-30 have a length of silicon nanowire 4.7 μm and 4.6 μm . Transmission loss in the frequency range of 8.2 – 12.4 GHz and transmission in 8 – 14 μm are given in Figure 2(a) and Figure 2(b), respectively.

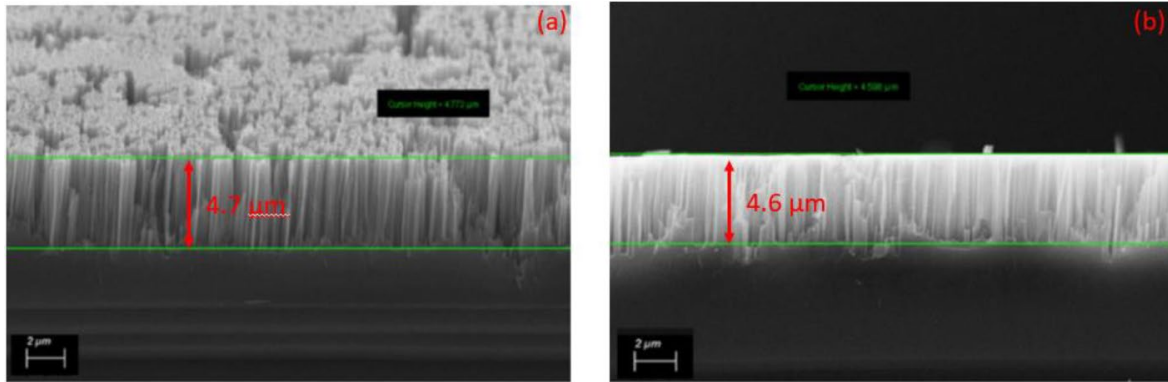


Figure 1: SEM images of the samples N-30 (a) and P-30 (b).

Numerically calculated transmission loss values of the samples were consistent with the experimental findings for both P-30 and N-30 samples in X-band. The average transmission loss of sample N-30 is -12.5 dB, and -7.2 dB for sample P-30 in X-band. In other words, samples N-30 and P-30 do not transmit the electromagnetic wave about 95% and 80% along the frequency range of 8.2 – 12.4 GHz. The difference between transmission values of the structures can be attributed to the different electrical conductivity.

Transmission of the non-textured reference samples and textured samples N-30 and P-30 in the LWIR band are shown in Figure 2(b). Non-textured reference samples have an average transmission of about 94% in the wavelength range of 8 – 14 μm , whereas the textured samples have a transmission of about 70%. This decrease in transmission can be attributed to light scattering between silicon nanowires. The electrical conductivity is the most probable reason for the slight difference in transmission between samples N-30 and P-30 in the LWIR band.

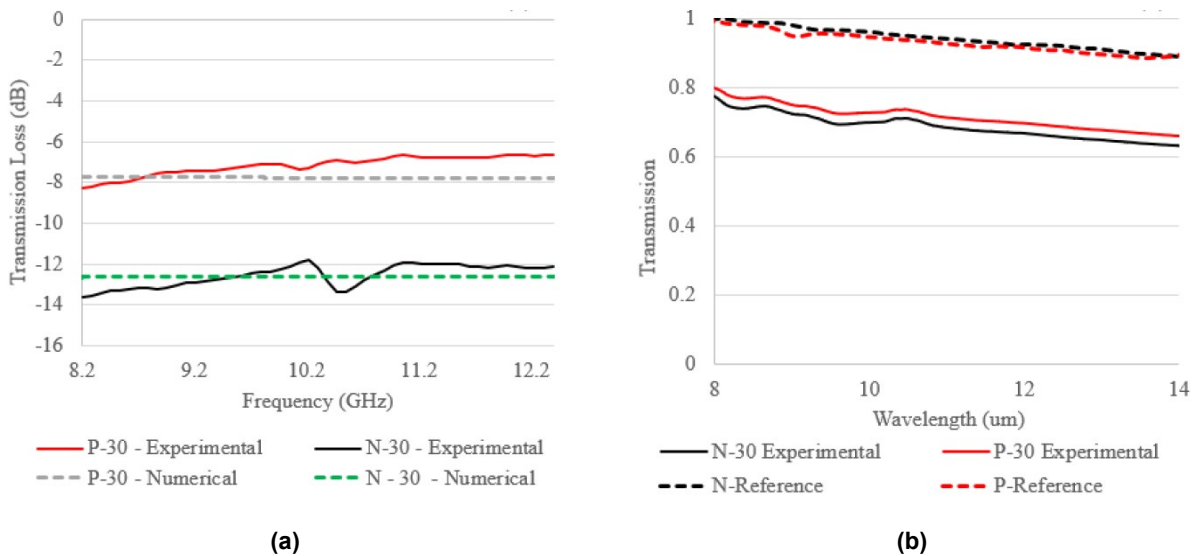


Figure 2: Responses of the textured silicon structures in X-band (a) and IR band (b).

4.0 CONCLUSION

In this study, we have fabricated textured silicon structures with similar texture types but different electrical properties. The fabricated structures were compared regarding their responses in the X-band and LWIR band. The results show that the structure's response for each band can be individually configurable by utilizing the length and electrical conductivity of silicon nanowires. In the future, numerical studies can be conducted to understand the behavior of the structures in the LWIR band. Additionally, ion implantation can be performed on the textured silicon structures to utilize electrical conductivity to enhance electromagnetic interference shielding.

ACKNOWLEDGEMENT

This work was partially supported by Scientific and Technological Research Council of Turkey (TUBITAK) under contract numbers of 5189901 and 20AG001. The authors are thankful for the collaboration between Turkish Aerospace and Bilkent University – UNAM. The authors are indebted to Dr. H. Volkan Demir, Dr. Alpan Bek and Gence Bektaş for their critical scientific recommendations.

5.0 REFERENCES

- Fuhrmann, B. et al. (2005). 'Ordered arrays of silicon nanowires produced by nanosphere lithography and molecular beam epitaxy', *Nano letters*. ACS Publications, 5(12), 2524-2527.
- Hu, Q. et al. (2003). 'High-frequency FTIR absorption of SiO₂/Si nanowires,' *Chemical Physics Letters*, 378(3-4), 299-304. doi: 10.1016/j.cplett.2003.07.015.
- Huang, Z. et al. (2011) 'Metal-Assisted Chemical Etching of Silicon: A Review,' *Advanced Materials*. John Wiley & Sons, Ltd, 23(2), 285-308. doi: <https://doi.org/10.1002/adma.201001784>
- Kern, W., 1990. The evolution of silicon wafer cleaning technology. *Journal of the Electrochemical Society*, 137(6), p.1887.
- Kim, Taehwan et al. (2016) 'Susceptibility of combat aircraft modeled as an anisotropic source of infrared radiation,' *IEEE Transactions on Aerospace and Electronic Systems*. IEEE, 52(5), 2467-2476. doi: 10.1109/TAES.2016.150513.
- Moghimi, M. J., Lin, G. and Jiang, H. (2018) 'Broadband and Ultrathin Infrared Stealth Sheets,' *Advanced Engineering Materials*, 20(11). doi: 10.1002/adem.201800038.
- Osminkina, L. A. et al. (2012) 'Optical properties of silicon nanowire arrays formed by metal-assisted chemical etching: Evidences for light localization effect,' *Nanoscale Research Letters*, 7, 1-6. doi: 10.1186/1556-276X-7-524.
- Saddiqi, N. et al. (2014) 'A Review on Synthesis of Silicon Nanowires by Laser Ablation,' *Chemistry and Materials Research*, 6(1), 76-86. Available at: <http://www.iiste.org/Journals/index.php/CMR/article/view/10329>
- Schmidt, V. et al. (2009) 'Silicon nanowires: A review on aspects of their growth and their electrical properties,' *Advanced Materials*, 21(25–26), 2681–2702. doi: 10.1002/adpma.200803754.
- Shimizu, T. et al. (2019) 'Effect of additives on preparation of vertical holes in Si substrate using metal-assisted chemical etching,' *Japanese Journal of Applied Physics*. IOP Publishing, 58(SD), SDDF06. doi: 10.7567/1347-4065/ab0ff5.

Wagner, R. S. and Ellis, W. C. (1964) 'Vapor-liquid-solid mechanism of single crystal growth,' Applied Physics Letters. American Institute of Physics, 4(5), 89-90. doi: 10.1063/1.1753975

Wolfsteller, A. et al. (2010) 'Comparison of the top-down and bottom-up approach to fabricate nanowire-based Silicon/Germanium heterostructures,' Thin Solid Films. Elsevier B.V., 518(9), 2555-2561. doi: 10.1016/j.tsf.2009.08.021

Zhang, R.-Q. (2014) 'Growth mechanism of silicon nanowires,' in Growth Mechanisms and Novel Properties of Silicon Nanostructures from Quantum-Mechanical Calculations. Berlin, Heidelberg: Springer Berlin Heidelberg, 7-12. doi: 10.1007/978-3-642-40905-9_2

